



Research Article

**CHARACTERIZATION OF AN EFFICIENT THERMAL INSULATION COMPOSITE SYSTEM FOR NON-RESIDENTIAL BUILDINGS: A COMPREHENSIVE THEORETICAL, NUMERICAL AND EXPERIMENTAL APPROACH**

**Giovanni Dipierro, Alessandro Massaro and Angelo Galiano**

Dyrecta Lab, IT Research Laboratory, Via VescovoSimplicio, 45, 70014 Conversano (BA), Italy

**ARTICLE INFO**

**Article History:**

Received 24<sup>th</sup> February, 2020

Received in revised form 19<sup>th</sup>

March, 2020

Accepted 25<sup>th</sup> April, 2020

Published online 28<sup>th</sup> May, 2020

**Key words:**

Thermal engineering, Thermal conductivity, Temperature measurement, Numerical analysis, Finite element analysis.

**ABSTRACT**

In this paper we investigate the thermal insulation efficiency of a novel concept of panelized wall system for non-residential buildings made of aluminium and polyvinyl chloride (PVC). The study is carried out by combining the results of 2D Finite Element Method (FEM) thermal and fluid dynamics numerical simulations, experimental data and theoretical investigations. According to the simulation results, technological aspects, theoretical and experimental data, we found a good thermal efficiency characterization of the double-chamber panels configuration. We theoretically investigate the thermal efficiency of the proposed system as a function of the distance between the panels and the wall to be insulated, finding that thermal insulation efficiency does not depend on the distance from the wall for gaps larger than about 3 cm. By combining the different approaches developed in this paper, we find a good agreement between theoretical, numerical and experimental results. This study demonstrates that the proposed methodology used to estimate and measure the heat transfer and the thermal efficiency, can be applied to different panels types made of different materials and in different configurations. The goal of the paper is to provide a guideline to model and to characterize the thermal isolation efficiency of panel.

Copyright©2020 **Giovanni Dipierro, Alessandro Massaro and Angelo Galiano**. This is an open access article distributed under the Creative Commons Attribution License, which permits unrestricted use, distribution, and reproduction in any medium, provided the original work is properly cited.

**INTRODUCTION**

Ensuring the effective thermal insulation of buildings is one of the key aspects of energy economy and environmental protection. In EU-27, there is an estimated air-conditioned area of 12.5 billion square meters and an average energy use of 159 TWh/year for heating and 7 TWh/year for cooling[1]. In particular, the reduction of energy demand in non-residential buildings, which represents 25% of the total stock in Europe and comprises a more complex and heterogeneous sector compared to the residential sector, is an important target to reach. Variations in usage pattern (e.g. warehouse versus workshops), energy intensity (e.g. lab rooms in hospitals versus to storage rooms in retail), construction techniques (e.g. industrial sheds versus office buildings) and the high demand for cost-effective, sustainable and easy to mount elements are some of the factors adding to the complexity of the sector. Nowadays, national codes for efficient energy usage require heat transfer values across external building walls to be lower than 0.3 W/m<sup>2</sup> K. Requirements or recommendations for this value may differ for different types of buildings, building age, etc. According to the European Directive 2010/31/EU (law 90/2013) all new (before 31/December/2020) buildings should be built with nearly zero energy consumption[2].

One of the first steps that can be pursued to reduce the energy consumption of a building is to improve insulation. In Italy, the maximum thermal transmittance allowed for the envelopes/walls of new buildings is 0.38 W/m<sup>2</sup> K in zone A and B and decreases towards the value of 0.22 W/m<sup>2</sup> K from zone C to zone F. In Table I are classified the climatic zones.

**Table I** Climatic zone classification

Zone	DD*
A	< 600
B	600 ÷ 900
C	901 ÷ 1.400
D	1.401 ÷ 2.100
E	2.101 ÷ 3.000
F	>3.000

\*DD (Days Degree): the Days Degree correspond to the sum, extended to all the days of the year, of the difference (only the positive one) between the temperature of the internal environment and the average daily external temperature (annex A of D.P.R. 26 August 1993 n.412 updated in the 2018).

Thermal insulation panels have been developed to reduce the heat transmission efficiency across the external walls of buildings, achieving a high level of thermal insulation and reducing the building's ecological footprint[3,4]. The use of one or more layers of insulating material on the opaque elements of the building envelope is a very common solution

\*Corresponding author: **Giovanni Dipierro**

Dyrecta Lab, IT Research Laboratory, Via VescovoSimplicio, 45, 70014 Conversano (BA), Italy

among the possible strategies to reduce energy requirements[5–7]. This method is mostly referred to as External Thermal Insulation Composite System (ETICS). Since the mid-1960s, ETICS have been adopted to increase the energy efficiency of buildings and represents the optimal solution for the energy efficient and sustainable thermal insulation of exterior walls and/or cladding in new construction as well as renovation. ETICS systems involve a multi-layer construction which is applied to the external facades of sheds. Typical materials used in this technique include polycarbonate, polystyrene, phenolic resin, polyurethane, mineral fibre, wood fibre and polyvinyl chloride (PVC) boards[8,9]

PVC is one of the world's most widely produced synthetic plastic polymer and its use is predominant in the construction industry due to its low production and installation cost, malleability and light weight. Due to its versatile nature, PVC has found applications across a broad range of industrial, technical and household uses. Among the main uses of this material, single-chamber (chamber indicates the air gap between each couple of layers constituting the panel) PVC panels are often used to clad shed's walls due its durability, low thermal conductivity and resistance to corrosion, moisture, abrasion or other forms of degradation[10]. Compared to polycarbonate, PVC is easier to find and offers a better thermal insulation (thermal conductivity of PVC is one order of magnitude smaller than the thermal conductivity of polycarbonate). Moreover, PVC boards are easier to fix on external walls (the time required to fix PVC sheet is around half of the one required to fix polycarbonate ones) due to its lower weight and can be easily painted and shaped. About three-quarters of all PVC produced goes into long-lasting building and construction applications. Although this material is intended to achieve high thermal performance, the conventional use of single-chamber PVC panels to clad sheds, however, is not optimal due to the long time required for assembly and the lower thermal insulation.

In this paper, we propose a prototypal thermal insulation composite system of PVC panels based on the thermal optimization of the commonly used single-chamber PVC panels to clad external buildings' walls. The optimization is aimed at ensuring a better thermal insulation keeping the same manufacturing and installation cost.

We investigate the energetic impact of the new system for the external thermal insulation of sheds and non-residential buildings in general, by carrying out numerical thermal simulations under dynamic conditions and steady state theoretical analysis of the heat transfer across external walls. In addition, we compare our theoretical and numerical results with experimental data finding a good agreement.

### Experimental setup

The prototypal thermal insulation composite system is made of a set of double-chamber rigid PVC panels. Each of the PVC layers is 2 mm thick and the three layers are evenly spaced between each other by 7 mm (the cross-section view is shown in Figure 1).



Figure 1 Cross-section view of the panel.

For experimental purposes, we built a representative sample of the system consisting in a reticular 250  $\times$  120 cm aluminium chassis composed by linear profiles embedding 12 rectangular 40 x 80 cm double-chamber PVC panels (

Figure 2). The PVC panels are anchored to the system thanks to an aluminium frame ensuring the required stiffness and a proper anchoring to walls ( Figure 3).

The insulation system is installed next to an existing brick wall, at 2.5 cm of distance from the. The system is held in place by a ground anchor made by aluminium. The anchors are designed for use with hollow brick walls and are placed on both sides to carry the panel load. Temperature sensors are installed to monitor the effectiveness of the insulation in the system. The sensors are located as shown in Figure 4.



Figure 2 Prototypal system of thermal insulation PVC composite panels.

The cluster of the three sensors (thermistors) is placed approximately at the center of the panel/wall. The aim is to measure the temperature:

- ✓ On the existing wall surface in the internal side of the building;
- ✓ On the exterior surface of the wall;
- ✓ On the exterior surface of the PVC panelized system.
- ✓ The purpose of these sensors is to monitor the temperature of both the surfaces of the wall surrounding the building to be insulated and the insulation panel itself. The monitoring system is connected to a control system which can be managed by means of an app available for both Android and iOS. Experimental data were collected every 15 minutes, starting from the 12<sup>th</sup> of December 2018 at 9:20 am and ending on the 5<sup>th</sup> of April 2019 at 01:35 pm. The data collection period allows to test the system in different environmental conditions.



Figure 3 Alluminium chassis embedding the 12 rectangular double-chamber PVC panels (see Fig. 2).

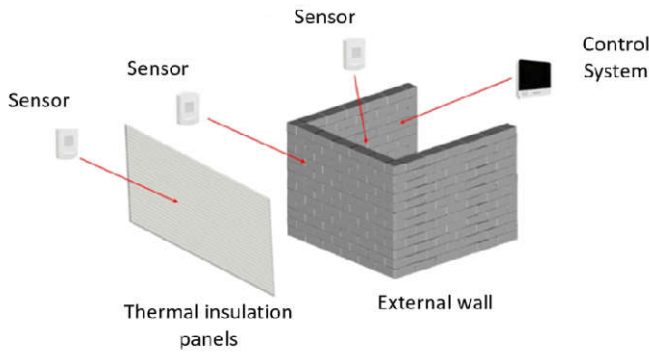


Figure 4 Temperature sensor locations

## RESULTS

Figure 5 shows the temperature of the internal (blue dots) and the external (green dots) surface of the wall with respect to the temperature measured on the exterior surface of the panel. Since, the temperature of the exterior surface of the panel is very close to the environmental temperature, we will hereafter refer to this value of temperature as ambient temperature.

The diagonal line shown in Figure 5 indicates the reference line to measure the efficiency of the thermal insulation. The farther away from the line the data are, the better is the thermal insulation provided by the system.

We note that the distribution of points is in accordance with our expectations: for ambient temperature lower than about 15 °C, the internal temperature of the building is larger by nearly 3 - 5 °C than the ambient temperature. On the other hand, for large ambient temperature (> 15 °C), the temperature of the internal part of the building is lower than the ambient temperature by a larger factor: 10 - 15 °C. This trend indicates that the insulation system performs properly, especially during warmer seasons (ambient temperature > 15 °C). In we will interpret these results using a theoretical approach.

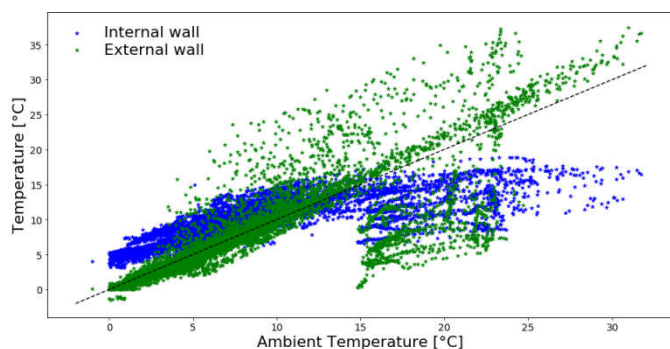


Figure 5 Temperature data of the internal part of the wall (blue) and on the exterior surface of the wall (green) vs ambient temperature. The dashed black

line indicates the diagonal line where the temperature values are equal to the ambient temperature.

### Numerical FEM Simulations of heat transfer

In order to support the design of the new composite system, we perform numerical Finite Element Method (FEM) simulations of heat transfer across the system[11,12]. The software Energy 2D (version 3.0.3) [13] is employed to investigate the thermal responses of the system, taking into account the heat transfer among the different components of the system and the dynamics of fluids involved in the numerical modelling. Energy 2D is an interactive, visual multi-physics simulation program that models the heat transfer across a variety of materials and fluids, allowing to simply test scientific hypothesis and solve engineering problems. In our case, the aim is to thermally characterize the efficiency of the proposed insulation panels installed close to a wall surrounding a building.

Our aim is to model the heat transfer across the insulation panels placed close to the external walls of a typical non-residential building. We consider a building as a room 50 m wide, 50 m long and 30 m high filled with air and surrounded by a 2.5 cm thick brick wall. In order to properly model the insulation panels described above, we consider 3 layers of PVC framed by an aluminium structure that surrounds each panel. As mentioned above in the description of the experimental setup (see Sect. 0), each layer of the insulation panel is  $L_{PVC} = 2 \text{ mm}$  thick and is spaced from the other layer by  $L_{air} = 7 \text{ mm}$ .

Due to the limitations of the software in handling large dynamical range in spatial dimension and bearing in mind that our aim is to model the heat transfer and characterize the thermal efficiency of the insulation panel, we consider a representative section of the system with a proper spatial scaling between the physical and numerical units.

We therefore model the building as a room 2.5 m wide, 2.5 m long and 1.5 m high filled with air and surrounded by a 2.5 m thick brick wall, in order to reduce the dynamical range of the spatial dimension of the different components of the system. All the spatial lengths mentioned above are expressed with the numerical units adopted in the software. We adopt proper values for the volume density, thermal conductivity and specific heat of the air inside the building by assuming that the linear size of the room is 20 times larger than the size modelled in our simulations. This allows us to model the heat transfer from a building with an active air volume of about 75000 cubic meters.

We place the insulation panels next to one of the side of the wall, while the other sides of the building are separated from the surrounding environment by a non-conductive material.

We numerically model the double-chamber PVC panel as a single object with thermal and physical properties given by the sum of the single properties of each of the three PVC layers and of the two air chambers between each pair. We therefore consider a single object with thickness equal to  $L_{equiv} = 3L_{PVC} + 2L_{air} = 2.5 \text{ cm}$  in physical units. In numerical units, since the physical width of the panel is an order of magnitude smaller than the external wall, we assume that the width of the panel is 0.25 m in numerical units. We remark that the sizes of the objects modelled in the software are set in order to ensure

the right proportion between the panel and the wall, while the size of the building is chosen for computational reasons, as described above.

We model the panels by adopting the standard physical and thermal properties of the PVC, i.e. mass density  $\rho_{PVC} = 1.3 \text{ g/cm}^3$ , thermal conductivity  $\lambda_{PVC} = 0.14 \text{ W/mK}$  and specific heat  $c_{PVC} = 900 \text{ J/Kg K}$ . The alluminium frame is modelled by assuming a mass density of  $\rho_{al} = 2.7 \text{ g/cm}^3$ , thermal conductivity  $\lambda_{al} = 237 \text{ W/mK}$  and specific heat  $c_{al} = 910 \text{ J/Kg K}$ . The wall is made of bricks with thickness  $L_{wall} = 30 \text{ mm}$  mass density  $\rho_{wall} = 1.75 \text{ g/cm}^3$ , thermal conductivity  $\lambda_{wall} = 0.442 \text{ W/mK}$  and specific heat  $c_{al} = 1000 \text{ J/Kg K}$ . The air in the environment where the system is placed is characterized by a mass density of  $\rho_{air} = 0.0012 \text{ g/cm}^3$ , thermal conductivity  $\lambda_{wall} = 0.026 \text{ W/mK}$  and specific heat at constant pressure at  $20 \text{ }^\circ\text{C}$  of  $c_{air} = 717.3 \text{ J/Kg K}$ . It is worth noting that, except for gases, the temperature and volume dependence of the specific heat of most substances is weak. For simplicity, we neglect the change in air specific heat with varying temperature, since the temperature values involved in this model do not change remarkably.

Since the insulation panels is numerically modelled as a single object, the thermal conductivity of the object is given by the combination of the five thermal conductivities of the layers (3 PVC layers and 2 air chamber). In detail, using the analogy with the Ohm's law in electromagnetic theory, we consider the equivalent thermal resistance given by the sum of the five resistances in series, i.e.

$$R_{equiv} = \frac{L_{equiv}}{\lambda_{equiv}} = \frac{3L_{PVC}}{\lambda_{PVC}} + \frac{2L_{air}}{\lambda_{air}}, \quad (1)$$

that can be used to compute the equivalent thermal conductivity:

$$\lambda_{equiv} = \frac{L_{equiv}\lambda_{air}}{2L_{air}+3L_{PVC}\frac{\lambda_{air}}{\lambda_{pvc}}} = 0.03 \text{ W/mK}. \quad (2)$$

The specific heat of the object is given by the sum of the specific heats of each layer.

We set the initial temperature spatial distribution for each of all the components of the system with the aim to create a thermal gradient between the building and the environment. The initial temperature of the building (including walls) is assumed to be equal to  $15 \text{ }^\circ\text{C}$ , while the initial temperature of the panels and the environment is set equal to  $0 \text{ }^\circ\text{C}$ . Figure 6 shows the geometry of the modelled system with colors showing the spatial distribution of temperature. We adopt the Dirichlet condition (constant temperature) for the temperature distribution at the boundary of the spatial domain, assumed to be large  $10 \times 10 \text{ m}$ . We note that the width of the spatial domain is large enough to avoid any influence of the boundary conditions on the results of the numerical simulations close to the system.

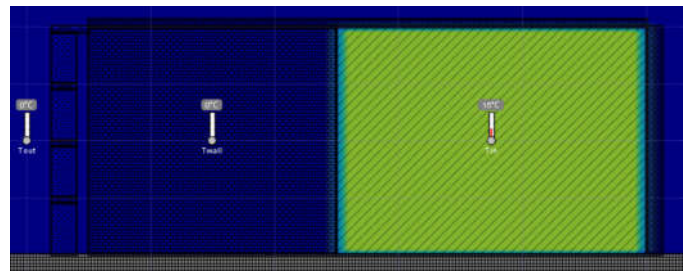


Figure 6 Rendered image of the initial temperature distribution of the system modelled in Energy2D.

We simulated the heat transfer among the different components of the system for 8 hours, allowing the system to approximately reach thermal equilibrium. It is worth noting that, since the temperature spatial distribution is not kept fixed along the simulations, the thermal equilibrium is reached when all the components of the system are at the same temperature. However, the thermal efficiency of an insulation system can be evaluated by analyzing the rate of heat transfer between the building and the environment along the simulations.

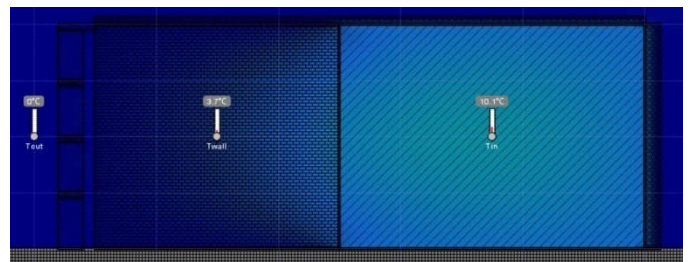
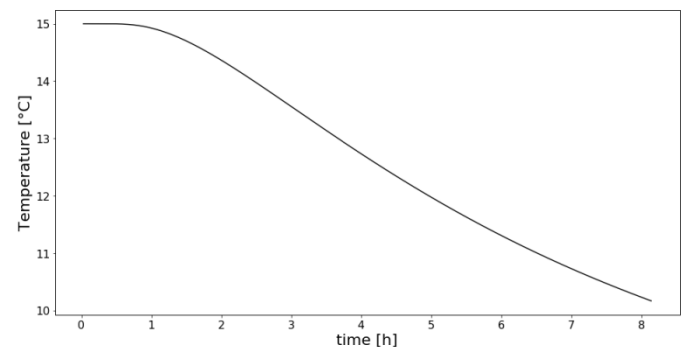


Figure 7 Rendered image of the temperature distribution of the system at the end of the simulation.

## RESULTS

Figure 7 shows the spatial distribution of the temperature in the system 8 hours after the beginning of the simulation. The temperature inside the building decreases from  $15 \text{ }^\circ\text{C}$  to  $10 \text{ }^\circ\text{C}$  due to the heat transfer across the wall and the panels. As expected, due to the large thermal inertia of the environment, the external temperature is equal to its initial value, i.e.  $0 \text{ }^\circ\text{C}$ .

Figure 8 shows the evolution of the temperature inside the building. After one hour from the beginning of the simulation, the temperature of the air inside the building decreases due to the heat flux across the walls. The decay rate of the temperature depends on the thermal conductivity of the panel and the wall and on the density and specific heat of the air inside the building. In Sect. IV we will interpret these results in terms of insulating power of the system using a theoretical approach.



**Figure 8** Time evolution of the temperature measure on the internal wall of the building.

### Theoretical Model

In this Section we analytically investigate the heat flux across the system in order give an estimate of the insulation power of the proposed two-chamber panel in stationary conditions.

We consider steady, one-dimensional (perpendicular to the panel and wall surfaces) heat flow through the panel (three PVC layers and two air chambers framed in an aluminium structure), the air layer between the panel and the wall and the wall itself in series, taking into account the influence of convection on both sides (environment and the interior part of the building). As described in Sect. 0, the system is made of 3 x 4 panels of height  $H_{PVC} = 40\text{ cm}$  and 3 small alluminium bars with height  $H_{al} = 1\text{ cm}$ . To vertically separate the system from the external environment, we consider an upper and lower anchor system made of an insulating material that prevents any air from seeping into the gap between the panel and the wall. For simplicity, we neglect the heat transfer through the anchor system, since we expect it will not contribute remarkably to the total thermal flux. We therefore compute the average heat flux across the system through conduction, convection and radiation taking into account its vertical stratification.

Using the analogy with the Ohm's law in electromagnetic theory, the PVC panels are assumed to be in parallel with the aluminium frame. Under steady condition, the Fourier's law of heat conduction gives the heat flux

$$\dot{Q} = \frac{T_{ext} - T_{int}}{\frac{1}{h_{out}} + \frac{1}{h_{int}} + R_{PVC+air+al} + \frac{L_{wall}}{\lambda_{wall}}}, \quad (3)$$

where  $T_{out}$  and  $T_{int}$  are the ambient temperature and the internal temperature of the building, respectively. The terms  $h_{out}$  and  $h_{int}$  are the convective heat transfer coefficients of the environment and the interior of the building, respectively. The term  $R_{PVC+air+al}$  indicates the thermal resistance of the panel and the air layer between the panel and the wall, given by:

$$R_{PVC+air+al} = \frac{R_{al} R_{equiv}}{4R_{al} + 3R_{equiv}} + \frac{L_{PVC-wall}}{Nu_{PVC-wall} \lambda_{air}}, \quad (4)$$

where  $R_{equiv}$  is expressed by Eq. 1,  $L_{PVC-wall}$  is the distance between the wall and the panel and  $R_{al} = f L_{equiv} / \lambda_{al}$ , with  $f$  indicating the ratio between the height of the PVC panel with respect to the height of aluminium frame:  $f = H_{PVC} / H_{al} = 40$ . The term  $Nu_{PVC-wall}$  is the Nusselt number of the air gap between the panel and the wall, defined as

$$Nu_{PVC-wall} = \begin{cases} 1 & \text{if } Ra < 2000, \\ 0.197 Ra^{1/4} \left( \frac{H_{tot}}{L_{PVC-wall}} \right)^{-1/9} & \text{if } Ra \in [2 \cdot 10^3, 2 \cdot 10^5], \\ 0.073 Ra^{1/3} \left( \frac{H_{tot}}{L_{PVC-wall}} \right)^{-1/9} & \text{if } Ra \in [2 \cdot 10^5, 10^7], \end{cases} \quad (5)$$

where  $H_{tot}$  is the vertical height of the system ( $H_{tot} = 4H_{PVC} + 5H_{al}$ ) and  $Ra$  is the Rayleigh number, i.e.

$$Ra = \frac{g \beta \Delta T L_{PVC-wall}^3}{\nu^2} Pr, \quad (6)$$

where  $g$  is the gravitational acceleration ( $9.81\text{ m/s}^2$ ),  $\Delta T$  is the temperature difference between the panel and the wall,  $\beta = 1/T_m$  where  $T_m$  is the average temperature between the panel and the wall,  $\nu$  is the kinematic viscosity and  $Pr$  is the Prandtl number, defined as the ratio of the diffusivity of linear momentum to the thermal diffusivity computed at the temperature  $T_m$ . We adopt the US Standard Atmosphere [14] for calculating viscosity of air as a function of the temperature.

It is worth remarking that we are assuming that the convection arises naturally without any influence from external effects (e.g. wind). Moreover, to simplify our analysis, we are assuming that the effect of the radiative heat transfer between the wall and inner side of the panel and among the different layers of the composite system is negligible.

The heat transfer coefficients between the wall and the air inside the building and between the panel and the environment are given, respectively, by:

$$h_{int} = \frac{\lambda_{air}}{H_{tot}} Nu_{int} + \epsilon_w \sigma (T_{int}^2 + T_{wallin}^2) (T_{int} + T_{wallin}), \quad (7)$$

$$h_{out} = \frac{\lambda_{air}}{H_{tot}} Nu_{out} + \epsilon_p \sigma (T_{out}^2 + T_{pout}^2) (T_{out} + T_{pout}), \quad (8)$$

where the second terms are the radiative heat transfer contribution with  $\epsilon_w$  and  $\epsilon_p$  indicating the emissivity of the wall ( $\epsilon_w = 0.92$ ) and the panel ( $\epsilon_p = 0.9$ ), while  $T_{wallin}$  and  $T_{pout}$  are the temperature of the interior surface of the wall and of the exterior part of the panel respectively.

The Nusselt number  $Nu$  in this case is defined by

$$Nu_{out/ext} = \left\{ 0.825 + \frac{0.387 Ra^{1/6}}{[1 + (0.492/Pr)^{9/16}]^{6/27}} \right\}^2, \quad (9)$$

where  $Ra$  is taken from Eq. 6 but replacing  $L_{PVC-wall}$  with  $H_{tot}$  and  $\Delta T$  with the temperature difference between the object's surface (exterior surface of the panel in the case of  $h_{out}$  and the interior part of the wall in the case of  $Nu_{int}$ ) and the environment with which the object transfers energy through convection (environment in the case of  $Nu_{out}$  and the interior part of the building in the case of  $Nu_{int}$ ). We compute the steady state thermal flux by assuming two different environmental conditions:  $T_{out,wint} = 0\text{ }^\circ\text{C}$  (winter season) and  $T_{out,summ} = 30\text{ }^\circ\text{C}$  (summer season). In both case, we assume  $T_{int} = 15\text{ }^\circ\text{C}$ , yielding to the same difference (in absolute value) between  $T_{out,wint/summ}$  and  $T_{int}$ .

Since to compute the Nusselt numbers we need to infer the temperatures of the surfaces, we use an iterative method that generates a sequence of improving approximate solutions of the heat flux until it converges to the exact solution. %Using the temperature values inferred by assuming these conditions, we compute better estimates of the convective coefficients and the heat flux across the system until the estimate converges to the exact solution.

The iteration method converges after a few steps giving the solution for the steady state heat flux in the case where  $T_{out} = T_{out,wint}$  is given by:

$$\dot{Q} = -4.12 \text{ W/m}^2, \quad (10)$$

while in the case where  $T_{out} = T_{out,summ}$ , we obtain

$$\dot{Q} = 4.31 \text{ W/m}^2, \quad (11)$$

We note that the thermal flux during summer is slightly larger than during the winter season.

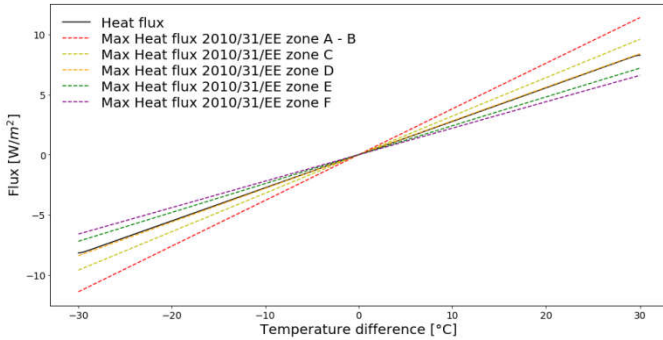


**Figure 9** Heat flux across the thermal insulation system varying the temperature difference between the building and the environment. Dashed lines indicate the requirements for the maximum heat flux according to the Directive 2010/31/EU for different Italian climatic zones.

In

Figure 9 we show the steady state thermal flux with different values of temperature differences between the building interior (assumed to be fixed to 15 °C) and the ambient temperature.

Comparing our results with the European requirements for the maximum thermal flux allowed for the new buildings (before 31/12/2020) in Italy according to the Directive 2010/31/EU, we find that the proposed system ensures a remarkable thermal insulation power and complies with the requirements of the new Directive for all the Italian climatic zones except zones E and F. This result suggests that the installation of the proposed system on the exterior walls of non-residential buildings can guarantee a better insulation according to the new European Directive.

### Changing the distance between the panel and the wall

Using the mathematical model developed in this paper we explore different configuration of the system by changing the distance between the panel and the wall.

Figure 10 shows that for distances smaller than about 3 cm, the heat flux increases with increasing distances from the wall. Importantly, for distances larger than about 3 cm, the heat flux is nearly constant with varying distances due to the fact that the convection becomes the dominant mechanism of heat transfer across the gap. becomes the dominant mechanism of heat transfer across the gap.

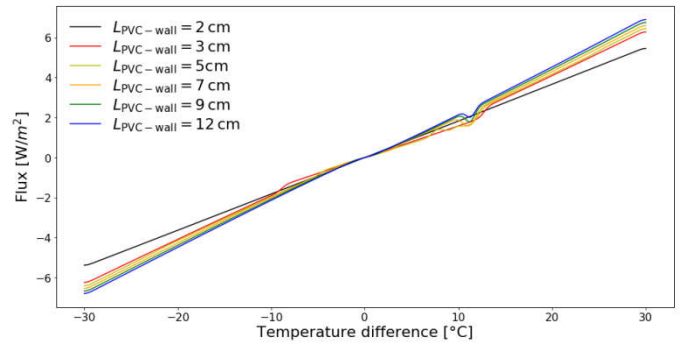


**Figure 10** Heat flux across the system with different distances between the wall and the thermal insulation system.

In detail, the influence of convective heat transfer depends on the difference between the Nusselt number  $Nu_{PVC-wall}$  defined in Eq. 5 and the unit value. When the convective heat transfer becomes dominant in the gap between the panel and the wall, the variation of the thermal resistance of that region with the width of the gap (second term on the right side of Eq. 4) becomes negligible. In detail, the term  $L_{PVC-wall}/Nu_{PVC-wall}$  depends very weakly with  $L_{PVC-wall}$  for  $Nu_{PVC-wall} > 1$ . By comparing the dependences of  $Nu_{PVC-wall}$  with the width of the gap, we obtain:

$$\frac{L_{PVC-wall}}{Nu_{PVC-wall}} \propto L_{PVC-wall}^\gamma, \quad (12)$$

with  $\gamma \in [0.11, 0.14] \ll 1$ . Therefore, the heat flux does not depend on the gap width when the convection becomes dominant, i.e. for gap width larger than about 3 cm.

Therefore, the heat flux does not depend on the gap width when the convection becomes dominant, i.e. for gap width larger than about 3 cm.

### Comparison between analytical and experimental results

The experimental results described in Sect. 0 can be interpreted using the theoretical model developed in Sect.0. We compare the temperature values measured on the external surface of the wall (green dots in Figure 5) with our theoretical expectations assuming stationary conditions. Starting from the temperature differences between the internal part of the wall and the environment obtained in our experimental campaign we compute the heat flux  $\dot{Q}$  by means of Eq. 3. The temperature of the external surface of the wall is therefore given by:

$$T_{wall} = T_{out} + \dot{Q} \left( \frac{1}{h_{out}} + R_{PVC+air+al} \right). \quad (13)$$

Figure 11 shows the comparison of the experimental data with our theoretical expectations. We note a good agreement between the theoretical values and experimental data, especially during the winter season. For large difference between the internal part of the building and the ambient temperature, the experimental results show larger dispersion in temperature with respect to theoretical expectations. This might be ascribed to a variety of reasons, such as the influence of wind (not taken into account in the theoretical analysis) that can affect the efficiency of convection.

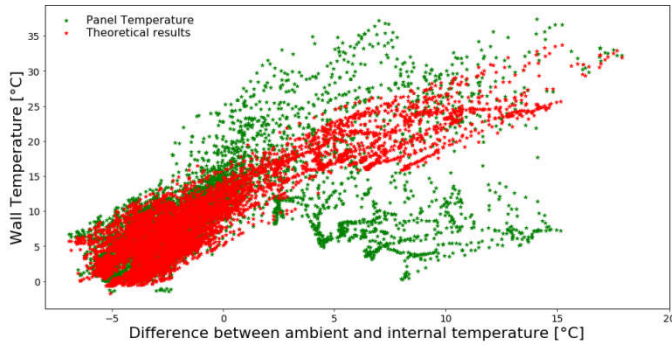


**Figure 11** Comparison between the experimental temperature of the exterior surface of the wall (green) and our theoretical expectations vs difference in temperature between the internal part of the building and the environment.

**Comparison between analytical and numerical results**

The theoretical model developed in this paper can be also useful to interpret the numerical results described in Sect.0[15,16].

The time decrease of the temperature inside the building can be modelled by using a lumped element method, assuming that the internal temperature of the building remains essentially uniform during the heat transfer process. The temperature of the air inside the building is thus assumed to be only a function of time  $T_{int}(t)$  while the thermal shield of the walls, the composite system and the environment are simply modelled as a single layer with thermal resistance given by:

$$R_{system} = \frac{1}{h_{out}} + R_{pvc+air+al} + \frac{L_{wall}}{\lambda_{wall}}, \quad (14)$$

where all the terms are described in Sect. 0.

Lumped system approximation provides a great convenience in heat transfer analysis and can be used if the internal thermal resistance (assumed to be equal to  $R_{int} = 1/h_{int}$  where  $h_{int}$  is expressed by Eq. 7) is negligible with respect to the external thermal resistance given by Eq. 14. We can assess the validity of this approach by computing a generalized version of the Biot number:

$$Bi = \frac{R_{int}}{R_{system}} \approx [0.01 - 0.1], \quad (15)$$

where the different values of  $Bi$  are computed by assuming a range in temperature of the internal building, the walls and the panels in the range [0-15] °C, since the thermal resistances of the components of the system depends on the temperature. Since the Biot number is  $\ll 1$ , we assume that the temperature inside the building is uniform during the heat transfer process and we can model the heat transfer between the building and the environment as follows:

$$\frac{mc_p}{A} \frac{dT_{int}}{dt} = \frac{T_{out} - T_{int}}{R_{system}}, \quad (16)$$

where  $m$  and  $c_p$  are the mass and specific heat at constant pressure of the air inside the building and  $A$  is the surface area across which the heat is transferred (surface area of the wall). Integrating Eq. 16 from  $t = 0$  where  $T_{int} = T_i$  to time  $t$ , we obtain the internal temperature as:

$$T(t) = T_{out} + (T_i - T_{out}) \exp\left(-\frac{AG}{mc_p} t\right), \quad (17)$$

where  $G$  is the thermal transmittance of the system surrounding the internal part of the building (walls, panel and environment), i.e.

$$G = \frac{1}{R_{system}}. \quad (18)$$

Eq. 17 shows that at time given by:

$$\tau = \frac{mc_p}{AG}, \quad (19)$$

the temperature is decreased to  $\approx 36\%$  of its initial time. This time, usually referred to as “decay time”, indicates the time needed to reach the thermal equilibrium between the system and the environment. According to this model, the temperature decrease follows an exponential decay. Assuming an external temperature of 0 °C and an initial temperature of the air inside the building of 15 °C, the value of the decay time of the temperature is  $\approx 7.7$  hours.

In the light of this, we thus fit the temperature time evolution shown in

Figure 8 with the exponential function expressed in Eq. 17 (see Figure 12) finding a scaling timescale of  $\approx 7.6$  hours (see legend in

Figure 12) which is consistent with the analytical value. To better compute the decay time, we run the numerical simulation for 30 hours, as shown in

Figure 12.

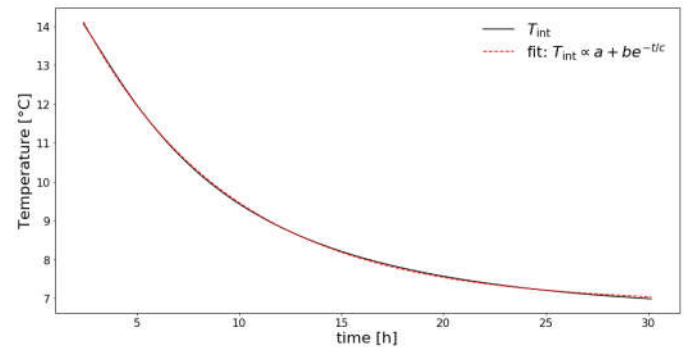


**Figure 12** Time evolution of the temperature inside the building. The dashed line represents the fit of the data with the exponential function shown in Eq. 17. Summary: Discussion and Insights

In this paper, we investigate the problem of the thermal characterization of a novel concept of thermal insulation composite system conceived for application in non-residential buildings (i.e. office and sheds). This system is made of a reticular aluminium framing structure embedding double-chamber PVC panels that constitute the insulating surface. We focus our analysis on a simplified prototype of this system covering just a delimited area of an external wall, realized and located at a fixed distance from it. A cluster of temperature sensors is placed in predefined position of the system, including also the internal part of the cladded wall in the scenario analysis. Data were collected at different times of the day and in different seasons of the year in order to give more meaningfulness to the results. Our results have shown that for ambient temperature lower than about 15 °C, the internal temperature of the building is larger by nearly 3 – 5 °C than the ambient temperature. On the other hand, for large ambient temperature ( $> 15$  °C), the temperature of the internal part of the building is lower than the ambient temperature by a larger

factor: 10 – 15 °C. This trend indicates the proper functioning of the insulation system, especially during warmer seasons (ambient temperature > 15 °C). Numerical Finite Element Method (FEM) simulations and a detailed analytical investigation have been carried out to support our analysis. We found that the thermal flux in summer is slightly smaller than in winter. Comparing our results to the European requirements for the maximum thermal flux for the new buildings (before 31/December/2020) in Italy according to the Directive 2010/31/EU, we found that the proposed system ensures remarkable thermal insulation power and complies with the requirements of the new Directive for all the Italian climatic zones except zones E and F. Finally, thanks to a mathematical model developed ad hoc for this work we find the heat flux does not depend on the gap width when the convection becomes dominant, i.e. for gap width larger than about 3 cm. Future studies could concern a more extended test of the thermal insulation system surrounding an entire non-residential building during a one-year period. Different thermal behaviors will be detected in this way even for the different wall exposures, allowing to realize the width of the air gap required from the thermal insulation system for each orientation. Infrared thermography (IRT) can be adopted to support experimental characterization, to check the surface panel temperature, and to characterize the aluminium adherence efficiency in terms of temperature homogeneity and thermal losses. In this direction IRT could optimize measurement protocols, by [17,18] Concerning the case of study have been acquired a thermo gram characterizing the aluminium chassis of the prototype (see Fig. 13 (a)). In order to focus the attention on the temperature behavior on the aluminium panel junctions have been filtered the radiometric image by enhancing temperatures below 32.4 °C (see red regions of Fig. 13 (b)). In the analyzed case a temperature inhomogeneities has been observed along the aluminium junctions: along some junctions such as L1 the temperature is strongly variable (see Fig. 14) by denoting possible thermal losses, besides along other junctions such as L2 the temperature is homogeneous thus confirming a correct panel assembly. For the radiometric measurement has been used FLIR T1020 having the following main specifications: thermal sensitivity <0,02 °C at 30 °C, IR sensor resolution of 1024 x 768 pixels, temperature range of -40°C to 2000°C, frame rate of 30 Hz, spectral range between 7.5 µm – 14 µm.

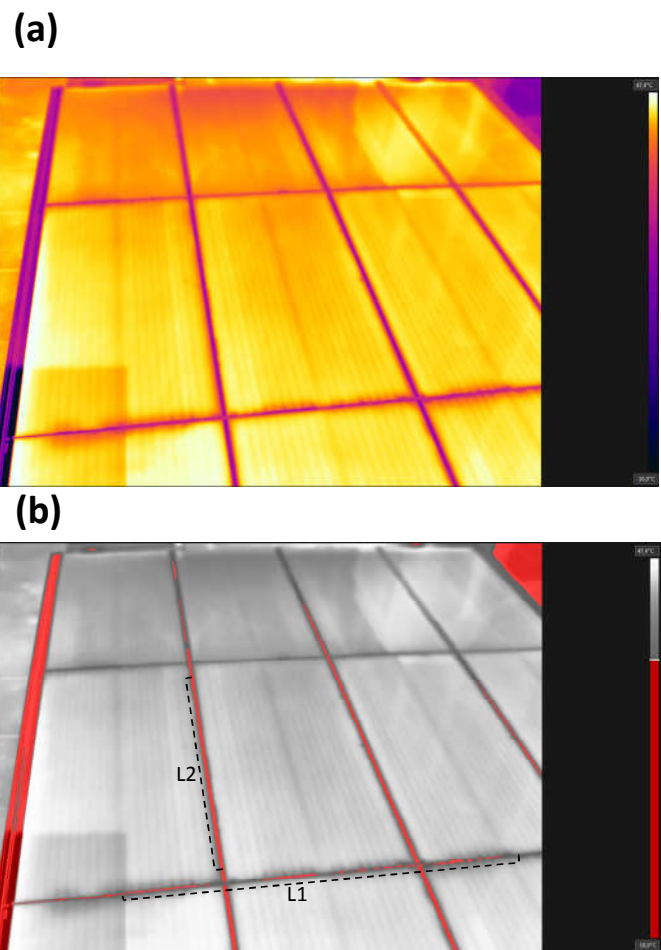


Figure 13 (a) Radiometric images of panels of Fig. 2. (b) Filtered regions below 32.4 °C and measurement line L1, L2 defined into the aluminium chassis of Fig. 3.

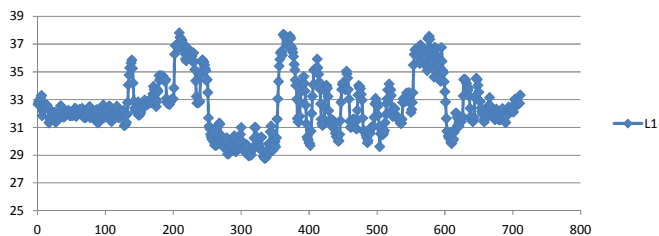


Figure 14 Temperatures trends along the measurement Line L1.

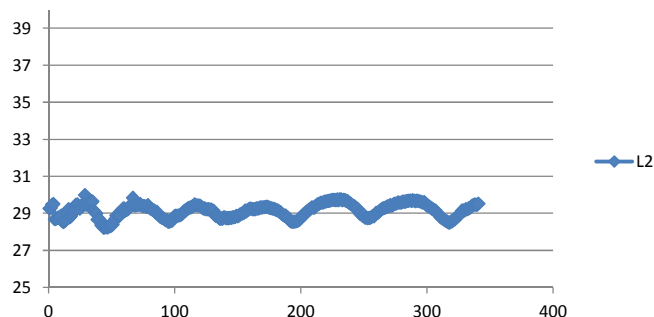


Figure 15 Temperatures trends along the measurement Line L2.

Finally, another important aspect to analyze is the steady/unsteady condition [19]. In this direction the provided theoretical model of Fig. 8 could provide the basic thermal behavior to compare for the thermal characterization of new panel materials.



## CONCLUSIONS

External thermal insulation composite systems make a significant contribution to increasing the energy efficiency of buildings. The use of two-chambers polyvinyl chloride insulating elements for energy retrofit of existing non-residential building envelopes is found to be a simple, attractive and potentially cost-effective option compared to the standard polycarbonate insulation panels. The paper is focused on the methodological approach to follow to characterize the thermal efficiency of PVC panels and chassis, by describing how to perform measurement and how to use temperature sensors including infrared thermography. The same approach can be adopted to each type of panels structured in different way and using different supports. The comparison between experimental and theoretical results suggests the formulation of a protocol to follow for the thermal characterization of panels. The discusses methodologies have been analyzed within the framework of an industry research project.

## Acknowledgments

The work has been developed in the frameworks of the Italian projects: “Infrastrutture meccanichee tecniche di montaggio ed ispezione per l’analisi dell’efficientamento energetico di pannelli applicabili ad edificio: Thermal Efficiency Model Panels” [‘Mechanical infrastructures and assembly and inspection techniques for energy efficiency of panels applicable on exterior walls of building: Thermal Efficiency Model Panels’]. Authors thanks for their effort the following Dyrecta Lab researchers: G. Birardi, A. Capasso, F. De Carlo, M. Legrottaglie, A. Lombardi, G. Lonigro, A. Lorusso, L. Maffei, N. Malfettone, A. Massaro, L. Patruno, L. Pellicani, R. Porfido, O. Rizzo, P. Scagliusi, M. Solazzo, D. Suma, E. Valenzano, and V. Vitti.

## References

1. BOLZANO AE DI. Survey on the energy needs and architectural features of the EU building stock, in: INSPiRE Project - Development of Systemic Packages for Deep Energy Renovation of Residential and Tertiary Buildings including Envelope and Systems. 2014.
2. Pérez-Lombard L, Ortiz J, Pout C. A review on buildings energy consumption information. *Energy Build* [Internet]. 2008;40:394–8. Available from: <https://linkinghub.elsevier.com/retrieve/pii/S0378778807001016>
3. Bouquerel M, Duforestel T, Baillis D, Rusaouen G. Heat transfer modeling in vacuum insulation panels containing nanoporous silicas—A review. *Energy Build* [Internet]. 2012;54:320–36. Available from: <https://linkinghub.elsevier.com/retrieve/pii/S0378778812003799>
4. Jang C, Kim J, Song T-H. Combined heat transfer of radiation and conduction in stacked radiation shields for vacuum insulation panels. *Energy Build* [Internet]. 2011;43:3343–52. Available from: <https://linkinghub.elsevier.com/retrieve/pii/S0378778811003860>
5. El-Darwish I, Gomaa M. Retrofitting strategy for building envelopes to achieve energy efficiency. *Alexandria Eng J* [Internet]. 2017;56:579–89. Available from: <https://linkinghub.elsevier.com/retrieve/pii/S1110016817301734>
6. Farmer D, Gorse C, Miles-Shenton D, Brooke-Peat M, Cuttle C. Off-the-Shelf Solutions to the Retrofit Challenge: Thermal Performance. *Sustain Ecol Eng Des* [Internet]. Cham: Springer International Publishing; 2016. p. 73–93. Available from: [http://link.springer.com/10.1007/978-3-319-32646-7\\_7](http://link.springer.com/10.1007/978-3-319-32646-7_7)
7. Cha J, Kim S, Park K-W, Lee DR, Jo J-H, Kim S. Improvement of window thermal performance using aerogel insulation film for building energy saving. *J Therm Anal Calorim* [Internet]. 2014;116:219–24. Available from: <http://link.springer.com/10.1007/s10973-013-3521-5>
8. Lu, John & Negulescu, Ioan & Wu Q. Thermal and Dynamic-mechanical Properties of Wood-PVC Composites. 2020;
9. Nagy B, Simon TK, Nemes R. Effect of built-in mineral wool insulations durability on its thermal and mechanical performance. *J Therm Anal Calorim* [Internet]. 2020;139:169–81. Available from: <http://link.springer.com/10.1007/s10973-019-08384->
10. Yousif E, Hasan A. Photostabilization of poly(vinyl chloride) – Still on the run. *J Taibah Univ Sci* [Internet]. 2015;9:421–48. Available from: <https://www.tandfonline.com/doi/full/10.1016/j.jtusci.2014.09.007>
11. Maile, Tobias & Fischer, Martin & Bazjanac V. Building Energy Performance Simulation Tools - a Life-Cycle and Interoperable Perspective. *Facil. Eng. (CIFE)*. 2007;
12. Younsi Z, Naji H. Numerical simulation and thermal performance of hybrid brick walls embedding a phase change material for passive building applications. *J Therm Anal Calorim* [Internet]. 2019; Available from: <http://link.springer.com/10.1007/s10973-019-08950-x>
13. Xie C. Interactive Heat Transfer Simulations for Everyone. *Phys Teach* [Internet]. 2012;50:237–40. Available from: <http://aapt.scitation.org/doi/10.1119/1.3694080>
14. States NU. U.S. Standard Atmosphere. 1976.
15. Nardi, Iole & Ambrosini, Dario & Paoletti, Domenica & Sfarra S. Combining Infrared Thermography and Numerical Analysis for Evaluating Thermal Bridges In Buildings: A Case Study. *Int J Eng Res Appl*. 2015;67–76.
16. Taylor T, Counsell J, Gill S. Combining thermography and computer simulation to identify and assess insulation defects in the construction of building

### How to cite this article:

Giovanni Dipierro, Alessandro Massaro and Angelo Galiano (2020) 'Composite System For Non-Residential Buildings: A Comprehensive International Journal of Current Advanced Research, 09(05), pp. 2217-2285. DOI: <http://dx.doi.org/10.24327/ijcar.2020.22185.4370>

\*\*\*\*\*

- façades. *Energy Build* [Internet]. 2014;76:130–42. Available from: <https://linkinghub.elsevier.com/retrieve/pii/S0378778814002175>
17. Massaro A, Galiano A. Infrared Thermography for Intelligent Robotic Systems in Research Industry Inspections. 2020. p. 98–125. Available from: <http://services.igi-global.com/resolvedoi/resolve.aspx?doi=10.4018/978-1-7998-0137-5.ch005>
18. A. Galiano, A. Massaro, D. Barbuzzi LP and VB. Heat Monitoring Plan in Building for Energy Efficiency using Thermal Imaging Analysis. *J Next Gener Inf Technol*. 2016;7:48.
19. Pavelek M, Adamová T. Bio-Waste Thermal Insulation Panel for Sustainable Building Construction in Steady and Unsteady-State Conditions. *Materials (Basel)* [Internet]. 2019;12:2004. Available from: <https://www.mdpi.com/1996-1944/12/12/2004>